JGR Earth Surface

RESEARCH ARTICLE
10.1029/2022JF006767

A Snapshot on the Buildup of the Stable Water Isotopic Signal in the Upper Snowpack at EastGRIP on the Greenland Ice Sheet

Alexandra M. Zuhr[1,2], Sonja Wahl[3], Hans Christian Steen-Larsen[4], Maria Hörhold[5], Hanno Meyer[1], and Thomas Laepple[1,6]

[1]Alfred-Wegener-Institut Helmholtz Zentrum für Polar- und Meeresforschung, Research Unit Potsdam, Potsdam, Germany, [2]Institute of Geosciences, University of Potsdam, Potsdam, Germany, [3]School of Architecture, Civil and Environmental Engineering, Ecole Polytechnique Fédérale de Lausanne, Lausanne, Switzerland, [4]University of Bergen and Bjerknes Centre for Climate Research, Bergen, Norway, [5]Alfred-Wegener-Institut Helmholtz Zentrum für Polar- und Meeresforschung, Research Unit Bremerhaven, Bremerhaven, Germany, [6]MARUM—Center for Marine Environmental Sciences and Faculty of Geosciences, University of Bremen, Bremen, Germany

Abstract The stable water isotopic composition in firn and ice cores provides valuable information on past climatic conditions. Because of uneven accumulation and post-depositional modifications on local spatial scales up to hundreds of meters, time series derived from adjacent cores differ significantly and do not directly reflect the temporal evolution of the precipitated snow isotopic signal. Hence, a characterization of how the isotopic profile in the snow develops is needed to reliably interpret the isotopic variability in firn and ice cores. By combining digital elevation models of the snow surface and repeated high-resolution snow sampling for stable water isotope measurements of a transect at the East Greenland Ice-core Project campsite on the Greenland Ice Sheet, we are able to visualize the buildup and post-depositional changes of the upper snowpack across one summer season. To this end, 30 cm deep snow profiles were sampled on six dates at 20 adjacent locations along a 40 m transect. Near-daily photogrammetry provided snow height information for the same transect. Our data shows that erosion and redeposition of the original snowfall lead to a complex stratification in the δ^{18}O signature. Post-depositional processes through vapor-snow exchange affect the near surface snow with d-excess showing a decrease in surface and near-surface layers. Our data suggests that the interplay of stratigraphic noise, accumulation intermittency, and local post-depositional processes form the proxy signal in the upper snowpack.

Plain Language Summary We study the process of the formation of the stable water isotope signal in surface snow on the Greenland Ice Sheet to better understand temperature information which is stored as a climate proxy in snow and ice. Our data consist of high-resolution surface topography information illustrating the timing and location of snowfall, erosion, and redeposition along a transect of 40 m, as well as stable water isotope records of the upper 30 cm of the snowpack sampled biweekly on 20 positions at the same 40 m long transect. The data cover a 2-month period during the summer of 2019. We find that the isotopic composition shows spatial variability of layers with low and high values, presumably winter and summer layers. We further observe that prevailing surface structures, such as dunes, influence the snow deposition and contribute to the found variable structure of the climatic information. Eventually, snow accumulation alone cannot explain all of the observed patterns in the isotopic data which is likely related to exchange processes between the snow and the atmosphere which modify the signal in the snow column after deposition.

Key Points:

- Combining digital elevation models and repeated snow sampling reveals the heterogeneous buildup of δ^{18}O signal in the snow column
- Surface structures (stratigraphic noise) substantially contribute to internal heterogeneity in δ^{18}O signature in the upper snowpack
- Proxy signals are formed in the surface layer by local processes, advected downwards with limited post-depositional influences below 10 cm

Supporting Information:

Supporting Information may be found in the online version of this article.

Correspondence to:

A. M. Zuhr,
alexandra.zuhr@awi.de

Citation:

Zuhr, A. M., Wahl, S., Steen-Larsen, H. C., Hörhold, M., Meyer, H., & Laepple, T. (2023). A snapshot on the buildup of the stable water isotopic signal in the upper snowpack at EastGRIP on the Greenland Ice Sheet. *Journal of Geophysical Research: Earth Surface*, *128*, e2022JF006767. https://doi.org/10.1029/2022JF006767

Received 24 MAY 2022
Accepted 1 FEB 2023

Author Contributions:

Conceptualization: Alexandra M. Zuhr, Hans Christian Steen-Larsen, Maria Hörhold, Thomas Laepple
Data curation: Alexandra M. Zuhr, Sonja Wahl, Hans Christian Steen-Larsen, Hanno Meyer
Formal analysis: Alexandra M. Zuhr, Thomas Laepple
Funding acquisition: Thomas Laepple
Investigation: Alexandra M. Zuhr, Sonja Wahl, Hans Christian Steen-Larsen, Maria Hörhold, Thomas Laepple

1. Introduction

Glaciers and ice sheets are a key component of the Earth's climate system. They are formed by deposition of snow through time which also builds up a chronology of climatic information. Stored information within stable water isotope records (e.g., δ^{18}O) from ice cores is commonly used as a paleoclimate proxy to infer past temperature variations (e.g., Brook & Buizert, 2018; Dansgaard, 1964; Jouzel et al., 2003).

While water isotopes are a proven proxy for temperature on long timescales and have been used to reconstruct continuous temperature series dating back ~800,000 years (EPICA Community Members, 2004), isotope profiles from Antarctica and Greenland depict a low signal-to-noise ratio (SNR) on annual to decadal temporal scales

Methodology: Alexandra M. Zuhr, Thomas Laepple
Supervision: Thomas Laepple
Validation: Alexandra M. Zuhr
Visualization: Alexandra M. Zuhr
Writing – original draft: Alexandra M. Zuhr
Writing – review & editing: Alexandra M. Zuhr, Sonja Wahl, Hans Christian Steen-Larsen, Maria Hörhold, Hanno Meyer, Thomas Laepple

(Fisher et al., 1985; Graf et al., 2002; Münch & Laepple, 2018) and individual records are poorly correlated to other records, even when the records are located within close vicinity to one another (Karlöf et al., 2006; Münch et al., 2016).

On local scales from several meters to hundred meters, snow is deposited spatially unevenly and final accumulation is primarily driven by depositional modifications of the initial snowfall. Driving processes are wind scouring, snowdrift, and redistribution that buildup characteristic surface features and influence the local accumulation (Fisher et al., 1985; Kuhns et al., 1997). This creates substantial heterogeneity between individual firn profiles (i.e., stratigraphic noise) (Fisher et al., 1985), and causes low correlations between adjacent firn or ice core records (Karlöf et al., 2006). The characteristics of this stratigraphic noise have recently been visualized and analyzed using density (Laepple et al., 2016; Weinhart et al., 2020) and isotopic data (Münch et al., 2016, 2017) from two-dimensional trenches in Antarctica.

The classical interpretation of the $\delta^{18}O$ signal in firn and ice cores assumes that the isotope signal reflects the signal of the snowfall (e.g., Lorius et al., 1969). It is further assumed that this signal is primarily affected by downward advection due to new deposited snow on top (Münch et al., 2017) and modified by densification and isotopic diffusion until the depth of firn ice transition (Johnsen, 1977; Johnsen et al., 2000). However, in recent years, the basic principle of this paleo-thermometer has been questioned (e.g., Casado et al., 2021; Town et al., 2008; Steen-Larsen et al., 2014). Studies show that the original isotopic composition of snow is considerably altered after the initial deposition by molecular exchange processes at the snow-air interface at and beneath the surface, including wind-driven ventilation, sublimation, vapor deposition, and snow metamorphism (Harris Stuart et al., 2021; Town et al., 2008; Wahl et al., 2021, 2022). Such modifications have been reported from laboratory experiments (e.g., Ebner et al., 2017; Hughes et al., 2021; Sokratov & Golubev, 2009) and observations from locations in Greenland (Steen-Larsen et al., 2014) and Antarctica (Casado et al., 2021; Ritter et al., 2016) with different accumulation rates.

To estimate the uncertainty introduced by stratigraphic noise and vapor-snow exchanges, to correct for the noise in climate variability estimates (Münch & Laepple, 2018), or to even use the heterogeneity as a proxy for past surface roughness (Barnes et al., 2006; Wolff et al., 2005), there is a need to characterize the driving processes accurately to parametrize and model them.

Here, we designed and performed a study to analyze for the first time the buildup of the isotopic signal in the upper snowpack over a summer season for a study site next to the deep drilling site of the East Greenland Ice-core Project (EastGRIP) in the accumulation zone of the Greenland Ice Sheet (GrIS). Based on previous studies and findings, we designed and performed an extensive two-dimensional snow sampling scheme making use of the liner technique (Schaller et al., 2016). Throughout the 2-months observation period, we sampled six 30 cm deep transects, sub-sampled them with 2 cm resolution, and analyzed the samples for their stable water isotopic composition. Additionally, near-daily digital elevation models (DEMs) for the same area were generated by applying an established Structure-from-Motion (SfM) photogrammetry technique (Zuhr et al., 2021) to quantify the changes in the snow surface height. The combination of both methods results in a unique data set that provides important information on the temporal evolution of the heterogeneity of the isotopic signal in firn and ice cores, as well as on near-surface post-depositional modifications.

2. Methods and Data

2.1. Study Site

A 40 m long transect was studied next to the EastGRIP campsite in northeast Greenland (75° 38′N, 36° 00′W, ~2,700 m altitude, Figure 1a) in the summer season of 2019. The site is characterized by an annual mean temperature of −29°C and prevailing westerly winds (Madsen et al., 2019). The studied transect was oriented perpendicular to the main wind direction with walking area being on the downwind side of the transect, following a similar setup as Zuhr et al. (2021). Annual accumulation rate estimates vary between 10 and 14 cm w.eq. yr^{-1} (Karlsson et al., 2020; Schaller et al., 2016; Vallelonga et al., 2014). Snow stratigraphy (e.g., specific surface area [SSA] and density) and atmosphere-snow exchange processes have been studied at the same location for the same observation period in Harris Stuart et al. (2021), Hughes et al. (2021), Wahl et al. (2021), and Wahl et al. (2022).

A nearby automatic weather station (AWS) from the Programme for Monitoring of the Greenland Ice Sheet (PROMICE) has been measuring meteorological data since 2015 (Fausto et al., 2021). During the observation

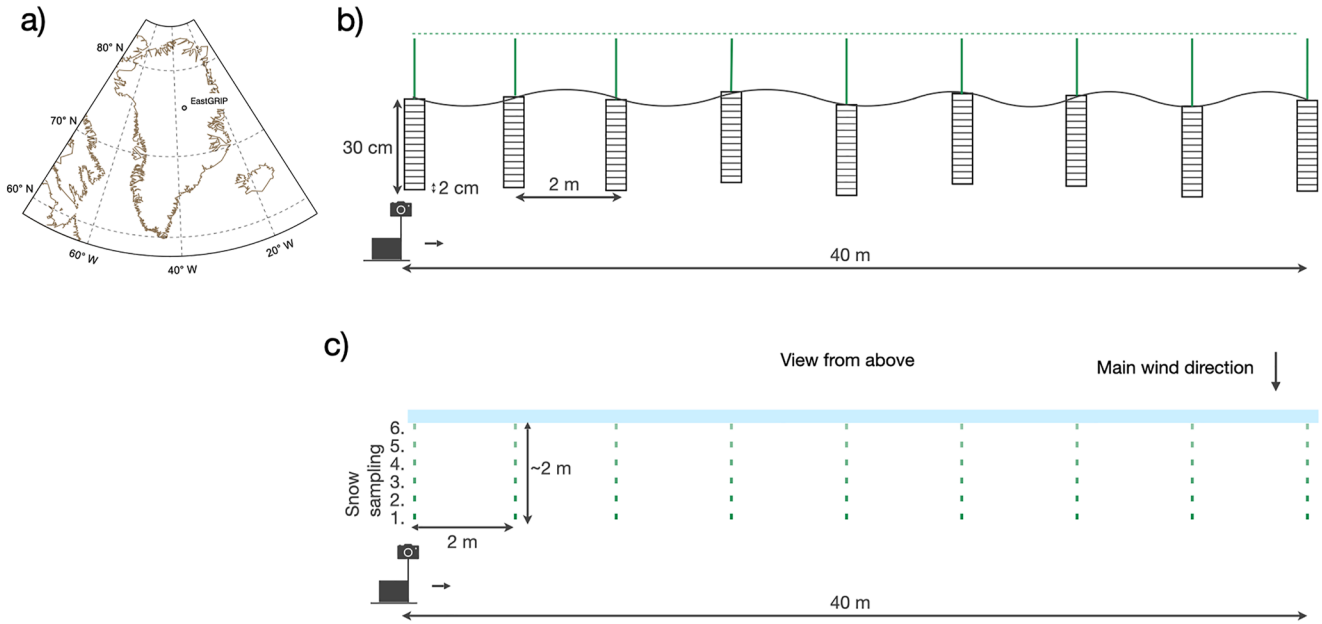

Figure 1. Location of the East Greenland Ice-core Project campsite (a) and illustration of the used setup for digital elevation model (DEM) generation and snow sampling (cross section view in b and from above in c). Along the 40 m transect, glass fiber sticks with 2 m spacing mark the snow sampling positions and were used as ground control points during the DEM generation (b). The horizontal dashed line indicates that all sticks were leveled to the same height. (c) Snow profiles were sampled at each stick position and had to move by about 30–40 cm with every sampling day. The blue area provides a representative snow height along the transect which was used to analyze the temporal evolution of the snow height and to simulate the signal content within the snow surface. For a better overview, the number of profiles and sticks is reduced in the sketch and does not represent the original setup.

period from 27 May to 27 July 2019, a mean temperature of −10.3°C and an average wind speed of 4.5 m s^{-1} mainly from the west (~240°, standard deviation of 46°) were observed (Figure 2a).

2.2. DEM Generation

Two-dimensional maps of the snow surface (i.e., DEMs) were generated for each day with suitable weather conditions to obtain detailed information on the snow height and its evolution throughout the observation period. For this, we carried out a SfM photogrammetry approach following the method established in Zuhr et al. (2021). Relative to their study, we used a Sony α 7R camera with a fixed lens of 35 mm focal length, mounted at a height of ~2 m (instead of ~1.5 m). Our DEMs have the same resolution of 1 cm × 1 cm while the improved setup enabled a larger coverage of 400 m^2 (= 40 m × 10 m) than the 195 m^2 in Zuhr et al. (2021).

At the beginning of the season, 20 glass fiber sticks with 2 m spacing were distributed along the 40 m long transect and used as ground control points for an absolute georeferencing (Figure 1b) (James & Robson, 2012). The DEM generation was carried out with the software Agisoft Metashape and the snow height at the first sticks on 27 May 2019 was defined as an arbitrary zero level to which all further DEMs were referenced. Due to the improvements of the setup, the accuracy of the DEMs should be equal (1.3 cm) or better than in Zuhr et al. (2021).

DEMs are available for 30 out of 62 days of the observation period providing an effective data coverage of 48%. Missing days are caused by cloudy and overcast conditions which impede the alignment of the photos. The largest gap between consecutive DEMs is 3 days and happened once. Gaps of 2 days occurred five times and a 1-day gap seven times. In case a DEM was not available for a day of snow sampling, a DEM from the day before or after was matched to the isotope profiles instead.

2.3. Isotope Measurements

To investigate the spatial and temporal evolution of the stable water isotopic composition of the upper firn layer, vertical snow profiles were collected at 20 positions with 2 m spacing along the 40 m transect on six days during the 2019 summer season (27 May, 6 June, 18 June, 3 July, 17 July, and 27 July 2019). The sampling distance is

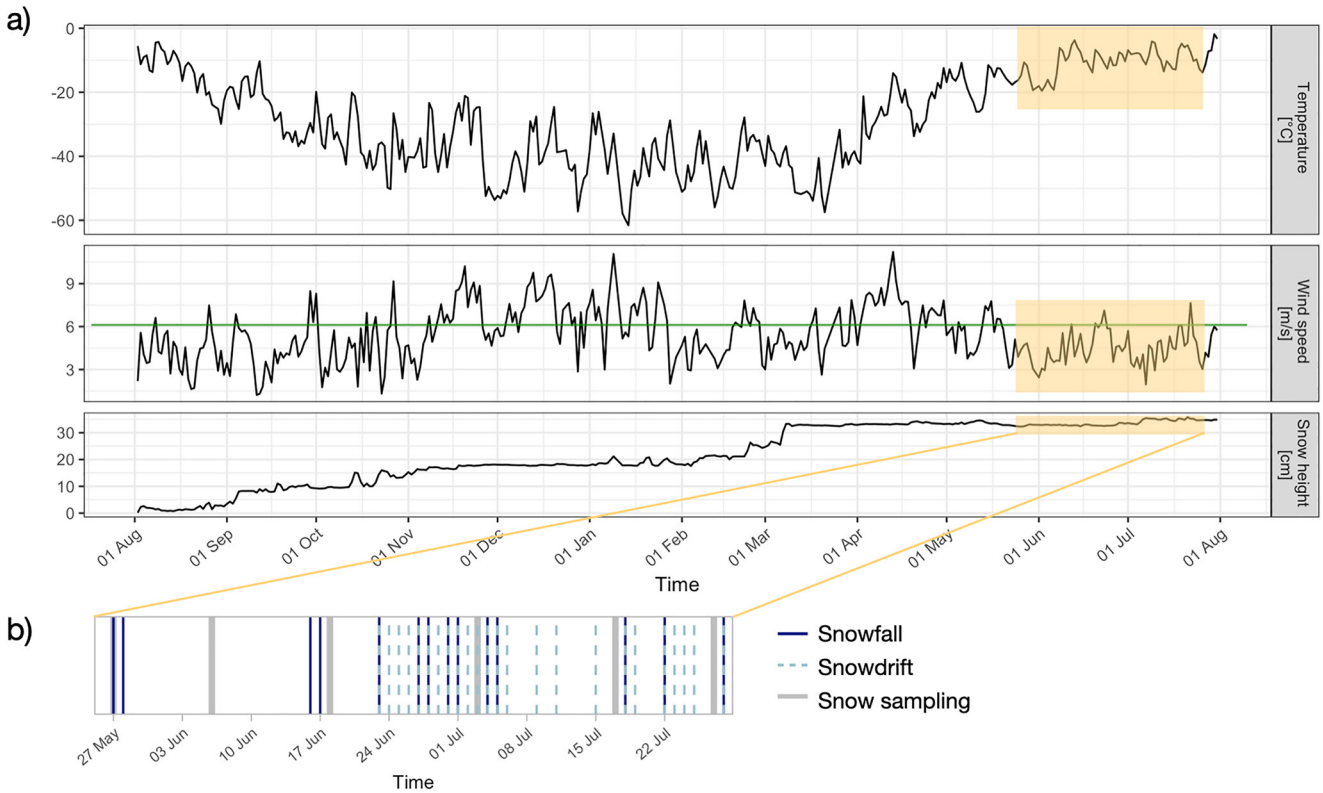

Figure 2. Meteorological observations showing (a) daily mean temperature, wind speed, and relative snow height from 1 August 2018 to 1 August 2019 measured at the Programme for Monitoring of the Greenland Ice Sheet automatic weather station. The horizontal green line denotes wind speed of 6 m s^{-1}, a typical threshold for snow erosion. The yellow areas mark the summer period covered in this study and for which manual observations of snowfall (in total 13×, dark blue) and snowdrift (in total 23×, light blue) are illustrated in panel (b) with an indication of the timing of snow sampling (gray bars).

small enough to resolve the scale of spatial variations in accumulation (Zuhr et al., 2021) and the length is a trade-off to capture some representative dune features while still being feasible to sample in a single day.

Carbon fiber tubes of 30 cm length and 10 cm diameter were used to collect mini-cores at each position (Figure 1c), following the liner technique described in Schaller et al. (2016). The sampling positions were filled with snow and flattened after each sampling to avoid disturbing surface features. Each position was moved by about 30–40 cm toward the main wind direction between successive samplings to avoid contamination from the previous sampling. The first and the last sampling positions were ∼1.8–2 m apart.

The mini-cores were cut immediately after the collection with a 2 cm vertical resolution, which is enough to resolve the isotopic variations as faster scales are damped by the isotopic diffusion. Depending on the recovered length of the snow cores (26–30 cm), the number of samples of single profiles varied between 13 and 15. The maximum sampled depth for single locations alternates between 26 and 30 cm of snow; thus, covering at least half a year of accumulation.

All snow samples were stored in airtight conditions in Whirl-Paks® and transported to Germany in a frozen state. Stable water isotope measurements were performed in the Stable Isotope Facility at the Alfred Wegener Institute in Potsdam, Germany, using a cavity ring-down spectrometer from Picarro Inc. (model L2140-*i*). Isotopic ratios are reported in the standard δ-notation given in per mil (‰) following

$$\delta = \frac{R_{\text{sample}}}{R_{\text{reference}}} - 1 \quad (1)$$

(Craig, 1961) with R_{sample} as the isotopic ratio of the sample and $R_{\text{reference}}$ the ratio of an in-house reference water calibrated against the international VSMOW/SLAP scale (Gonfiantini, 1978). All data were corrected for memory and instrumental drift as suggested in van Geldern and Barth (2012) using the calibration algorithm described in

Münch et al. (2016). The mean measurement uncertainty derived from an independent quality control standard was 0.13‰ and 1.4‰ for δ^{18}O and δD and for all used reference waters 0.09‰ and 0.7‰, respectively. Additionally, the second-order parameter deuterium-excess was calculated from the data following

$$\text{d-excess} = \delta D - 8 \cdot \delta^{18}O. \quad (2)$$

2.4. Simulation of the Snowpack Layering

To interpret the buildup of the internal isotope signal and the imprinted temperature information within the snowpack, we simulate the expected layering using the near-daily snow height information from the DEMs and the temperature data from the nearby AWS. We perform this simulation only for the δ^{18}O signal as this is the isotope species which is commonly used as paleoclimate proxy. Following the classical paleo-thermometer concept, we use mean daily temperature as a proxy for the signal in the new accumulated snow. Thus, the model provides the expected internal δ^{18}O structure of the snow column.

We extract the DEM-derived snow height for a 20 cm wide field behind the sampling locations (Figure 1c, blue area) and use it as a representation for the evolution of the mean snow height along the 40 m transect. This area is chosen because it is well-covered by the DEMs, close to the sampling positions (within 2 m) and, hence, representative of the snow height evolution at the sampling spots while not disturbed by the sampling itself. Using this snow height information, we simulate the expected internal δ^{18}O structure of the upper snowpack, similar to Figure 11 in Zuhr et al. (2021), by assigning the daily mean temperature to the respective day-to-day change in the snow height. We also account for snow erosion by considering negative changes in the snow height, but we do not consider density or density changes within the top 30 cm of the snow column as it has been shown to be almost constant over depth within the first meter (Schaller et al., 2016).

We perform this simulation for each day with available DEMs, starting on the day after the first sampling, that is, 28 May 2019, and show the results for the same following five days at which the snow sampling was performed. To qualitatively compare the simulated two-dimensional structure, which is still in temperature units, to our observed stable oxygen isotope profiles, we manually adjust the color-scales. We do not transfer the temperature to isotopic values since the temporal slope cannot be determined with the temporally limited data set. The comparison is not affected by this, because it would not change the correlation due to the linear character of the calibration. Furthermore, we do not simulate d-excess because we do not account for any depositional or post-depositional changes which we expect to influence d-excess.

2.5. Expected Uncertainty Due To Changes in the Sampling Position

To study the temporal evolution of a snowpack, it would be desirable to sample the same place and exactly the same snow at each time step. This is, however, not possible due to the destructiveness of snow sampling. Thus, sampling positions were moved each time by 30–40 cm toward the main wind direction, that is, perpendicular to the transect, to avoid disturbances (Figure 1c). As we move the sampling positions with time, we have to consider the heterogeneous character of surface snow (Münch et al., 2016, 2017). At the end, the first and last sampling locations are ∼2 m apart, similar as the spacing between two adjacent sampling positions. As a measure of the expected isotope variability, we first calculate the differences in the parameter between adjacent profiles as a function of sampling depth. We then calculate the standard deviation of the differences of each profile pair independent of depth. The mean of all standard deviations accounts to 2.9‰ for δ^{18}O and 2.5‰ for d-excess. These values represent the expected uncertainty due to changes in the sampling position. Hence, we cannot detect any significant change in the δ^{18}O data smaller than 2.9‰ or 2.5‰ in the d-excess data.

3. Results

3.1. Snow Height Evolution

The snow height along the transect is illustrated for each day (Figure 3) and shows an overall increase of ∼6 cm from the end of May to the end of July 2019. This increase is, however, not spatially uniform and influenced by precipitation intermittency and snow redistribution as indicated by manual observations of snowfall and snowdrift (Figure 2b). While the (net) snow accumulation exceeded 10 cm snow height change at few locations (e.g.,

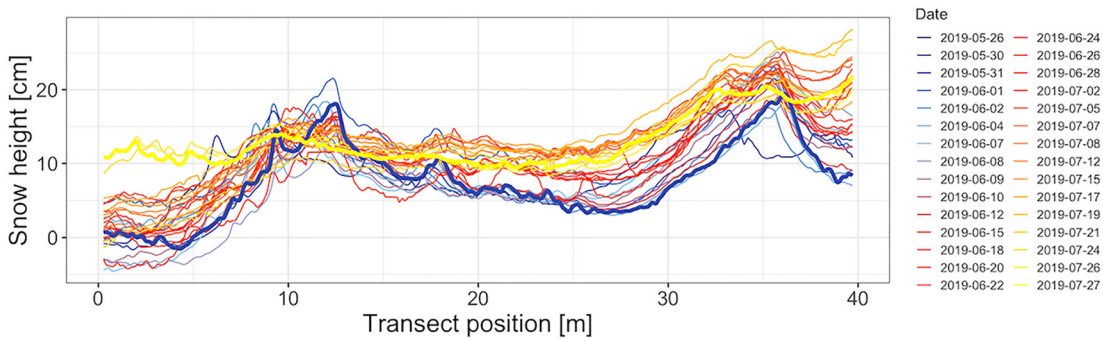

Figure 3. Temporal evolution of the digital elevation model-derived snow height (20-point running mean) along the 40 m transect. The color code indicates the day throughout the observation period from blue representing end of May via red to yellow indicating end of July. The bold lines in blue and yellow denote the first (27 May 2019) and last sampling day (27 July 2019), respectively.

at the positions 2, 38 and 40 m), other spots accumulated none or very less new snow (e.g., the positions at 12 and 36 m). Comparing the first (Figure 3, blue line) and the last (yellow line) day of the sampling period shows a flattening of the surface topography over time as troughs (between 0 and 10 m, 18 and ∼32 m, and between 37 and 40 m) are filled preferentially and receive more snow than the local elevation maxima at ∼13 and 36 m. Further, we also observe decreases in the snow height between consecutive days, indicating snow erosion. The dune between 11 and 14 m in the beginning of the observation period is eroded and/or sublimated with time. Similarly, the second dune between 32 and 38 m first becomes more pronounced before erosion and/or sublimation flattens this feature toward the end of July.

3.2. Mean δ^{18}O Records

Mean δ^{18}O values across all profiles increase from −38.3‰ on 27 May to −35.8‰ on 3 July, followed by a decrease to −36.3‰ toward the end of July 2019 (Figure 4, dashed vertical lines) with δ^{18}O values of individual samples ranging between −57.0‰ and −21.9‰ across all sampling days. The mean δ^{18}O profile on 27 May 2019 is characterized by a local isotopic minimum at ∼9 cm sampling depth (Figure 4). Toward the end of July, this layer is found at 17 cm depth with almost no change in the δ^{18}O value, roughly in agreement with what we expect from the observed 6 cm accumulation of new snow and the accompanying downward advection of the snow. Throughout June and July, the lowest mean value for a sampled depth changed from −42.5‰ to −41.4‰. We assign this part of low δ^{18}O values to the winter period (December to March, Figure 2a). On each sampling day, the highest δ^{18}O value is always found at the surface and increases with time due to the deposition of

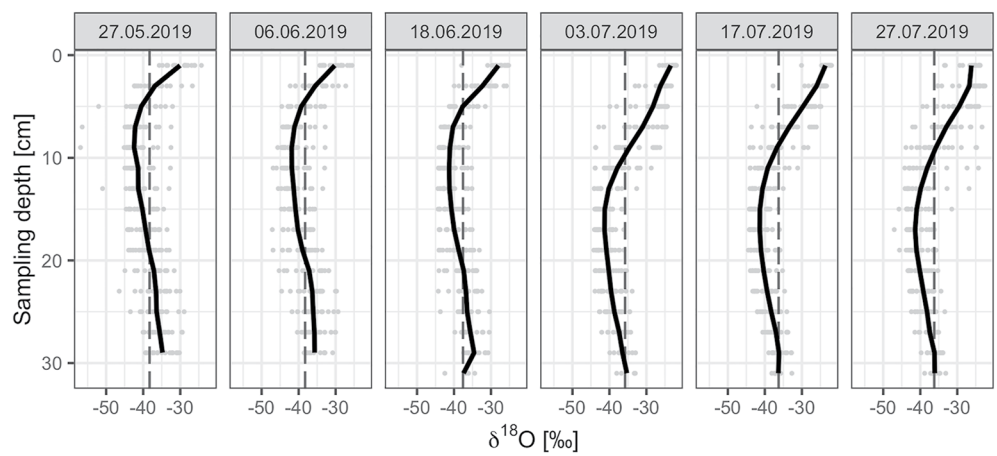

Figure 4. δ^{18}O profiles versus sampling depth for each of the six sampled days. Individual samples (gray points), the mean across sampling depth (black line) as well as the overall mean δ^{18}O value for each day (dashed vertical line) are indicated. No correction for downward advection due to new snow accumulation is performed.

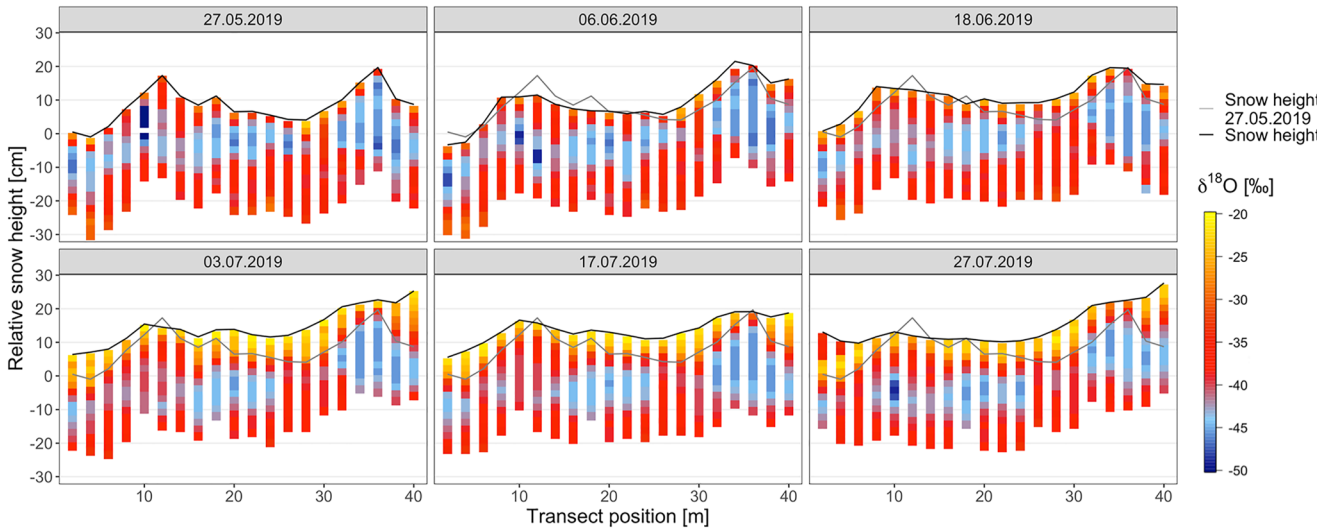

Figure 5. Two-dimensional view on the $\delta^{18}O$ variability of each profile on a respective sampling day aligned with digital elevation model-derived snow height information. The black line indicates the relative snow height for each individual sampling day and the gray line the snow height of the first sampling day, that is, 27 May 2019. Transect position corresponds to the distance along the transect (Figures 1b and 1c).

new, isotopically enriched snow throughout the summer period and/or due to sublimation-induced enrichment of surface snow (Figure 4, gray dots). The mean $\delta^{18}O$ values for the upper most 2 cm across all 20 sampling locations rose from −30‰ in May to −23.4‰ in July 2019.

3.3. Combining Isotopic Data With Snow Height Information

Analyzing the two-dimensional temporal sampling in combination with snow height information offers insights into the spatial and temporal $\delta^{18}O$ variability (Figure 5). On 27 May, the transect was characterized by a layer with depleted $\delta^{18}O$ values between −47‰ and −42‰ with a local minimum in the profile at 10 m (Figure 5, dark blue). The vertical extent of this depleted layer varies between 5 and 10 cm within most profiles. However, the profile at 36 m has an exceptionally large vertical extent of ∼24 cm, while the nearby profiles at 28 and 30 m do not show this layer at all. The depleted layers were mostly surrounded by isotopically more enriched layers and represented the winter layers as mentioned in Figure 4 and Section 3.2.

The relative depth of the depleted $\delta^{18}O$ values changes over time due to a downward advection from new snow accumulation whereas the layers themselves, such as the depleted area between 10 and 25 m, change only slightly. The low $\delta^{18}O$ values between 30 and 40 m are noteworthy because they remain quasi constant and only show slight changes with on an average 1.1‰ during the observation period (Figure 5).

The amount of the successively deposited snow in the upper layers corresponds to the thickness of the difference in snow height as observed in the DEMs (Figure 5, gray line indicates the first sampling day). The change in snow height between the first and the third sampling, that is, from 27 May to 18 June, indicates a gradual filling of the trough between 15 and 27 m with the deposition of snow with slightly enriched $\delta^{18}O$ values with on average −30.2‰. In contrast, the new layers on 3 and 17 July, defined via changes in the snow height, indicate a deposition of strongly enriched mean isotopic ratios of −25.1‰ and −23.6‰, respectively, and a continued flattening of surface undulations. This snow stayed until the end of July. The last sampling day showed a locally constrained accumulation with more negative values in a corner between 2 and 4 m and with similar $\delta^{18}O$ values than the previous depositions between 36 and 40 m.

The second-order parameter d-excess can provide additional information on the climatic signal contained in the upper snowpack (Figure S1 in Supporting Information S1). Overall, the mean d-excess decreased from 10.8‰ on 27 May to ∼8‰ for the last three samplings with single profiles showing an increase in d-excess from the surface downwards. The overall standard deviation increased slightly from 4.4‰ to 5.4‰ throughout the observation period. Individual sample values down to −10‰ are observed at and close to the surface on 17 and 27 July, corresponding to enriched $\delta^{18}O$ values in the same samples. However, the d-excess data are spatially more

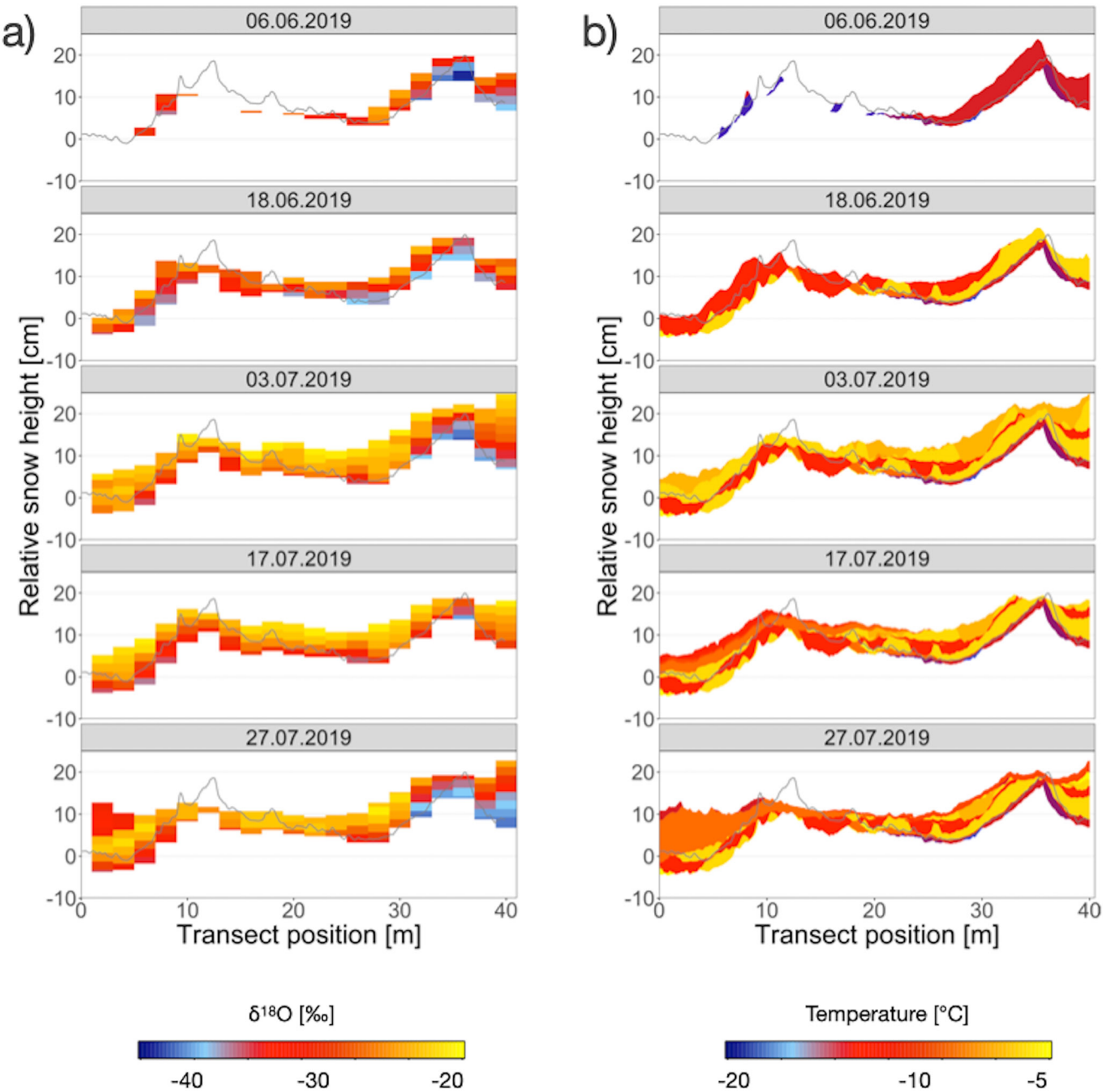

Figure 6. Two-dimensional view of the internal structure of the newly deposited snow from (a) observations and (b) simulations using digital elevation model (DEM)-derived snow height information and daily temperatures from the nearby automatic weather station. The $\delta^{18}O$ observations in panel (a) denote the newly accumulated snow during the observation period. The simulation in panel (b) assigns the daily temperature to all positions which received accumulation on a given day. The thickness might be influenced by missing DEMs (largest gap is 3 days) which could lead to a slightly overestimated thickness of specific layers. The gray line indicates the snow height on the first day of sampling.

homogenous compared to $\delta^{18}O$ and do not reproduce the observed patchiness in $\delta^{18}O$ data with the pronounced winter layer.

3.4. Observed Versus Simulated $\delta^{18}O$ Composition

A better understanding of the buildup of the upper snowpack can be achieved by visually comparing the observed stable oxygen isotopic composition (Figure 6a) with the expected precipitation-weighted temperature (Figure 6b) within the two-dimensional transects. This comparison will enable us to distinguish between changes due to

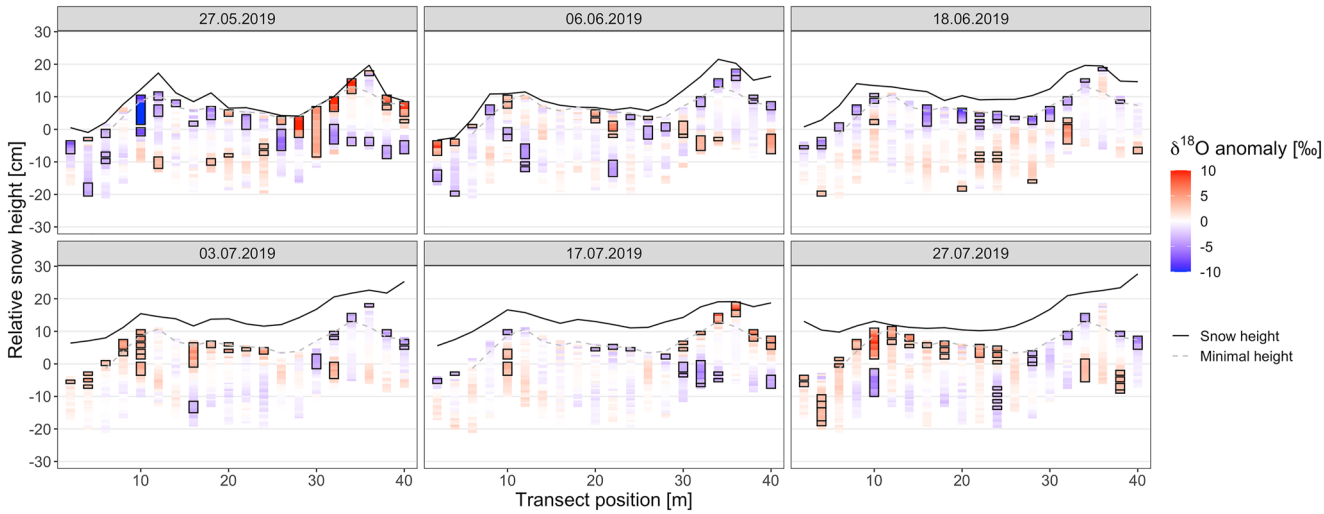

Figure 7. Anomalies of the mean δ^{18}O composition for each sample. Only sample positions are considered which have a value on each sampling day. New snow accumulation is therefore not included. Black squares indicate significant anomalies, that is, larger deviations than twice the local uncertainty of 1.45‰. The dashed gray line indicates the lowest snow height observed during the entire observation period and the black line the snow height for each sampling day, respectively.

depositional processes (redistribution, erosion or new deposition) and post-depositional modifications of the snow (vapor-snow exchange).

The δ^{18}O data suggests that the accumulated snow throughout the observation period represents several snowfall events with spatially heterogeneous layer thicknesses (Figure 6a). In the beginning of July, for example, most of the surface snow is characterized by layers of strongly enriched snow up to −21.9‰. This layer persists for several weeks, especially at the positions between 0 and 30 m. Similar features are found in the expected temperature content as shown by the simulations (Figure 6b). On 27 July, however, the area between 0 and 6 m indicates differences between the observed isotope ratios and the simulated internal layers from DEM-derived snow height changes.

3.5. Seasonal Evolution of the Snow Isotopic Composition

The presented analysis suggests that the main changes of the δ^{18}O signal through time is the addition of snow with a distinct isotope signature at the surface or a retrieval of material via wind-driven uptake and redeposition. To test whether the δ^{18}O signal is also changing over time in the depth range not directly affected by accumulation or erosion, we analyze the isotope anomaly maps in the zones that were not eroded at any point during the two months (Figure 7, dotted line) after removing the time-mean two-dimensional isotope profile (Figure 7).

Even if no change in the isotopic composition in a given snow parcel would have occurred, we would expect some variations due to the horizontal changes in the sampling position and, thus, sampling a new snow column every day. As the changes in the horizontal sampling position relative to the mean position is less than 1 m (i.e., half of the 2 m spatial range), we use 2.9‰ (two times the expected standard deviation for a 1 m horizontal shift) as a heuristic threshold for local significant δ^{18}O changes not attributed to spatial heterogeneity.

In general, more than 86% of the δ^{18}O anomalies are within ±2 SD (i.e., 2.9‰, Figure 7) suggesting that only some locations show changes not explainable with spatial heterogeneity. Stronger changes are observed closer to the surface while changes further down in the snowpack are weaker. Whereas the sign of change seems systematic near the surface from negative anomalies in the beginning of the season to positive anomalies at the last sampling, the sign of the changes further down in the snow column is varying.

In contrast to δ^{18}O, d-excess is highly sensitive to non-equilibrium processes (Casado et al., 2021). Thus, d-excess is often assumed to be primarily governed by the environmental conditions during evaporation at the moisture source region (e.g., Merlivat & Jouzel, 1979; Pfahl & Sodemann, 2014) making it a key constraint for temperature reconstructions when accounting for moisture source region changes (e.g., Landais et al., 2021).

For this analysis we combine information of snow present throughout the whole season and new snow being accumulated throughout the season and compute the observed changes between sampling events (Figure 8). We

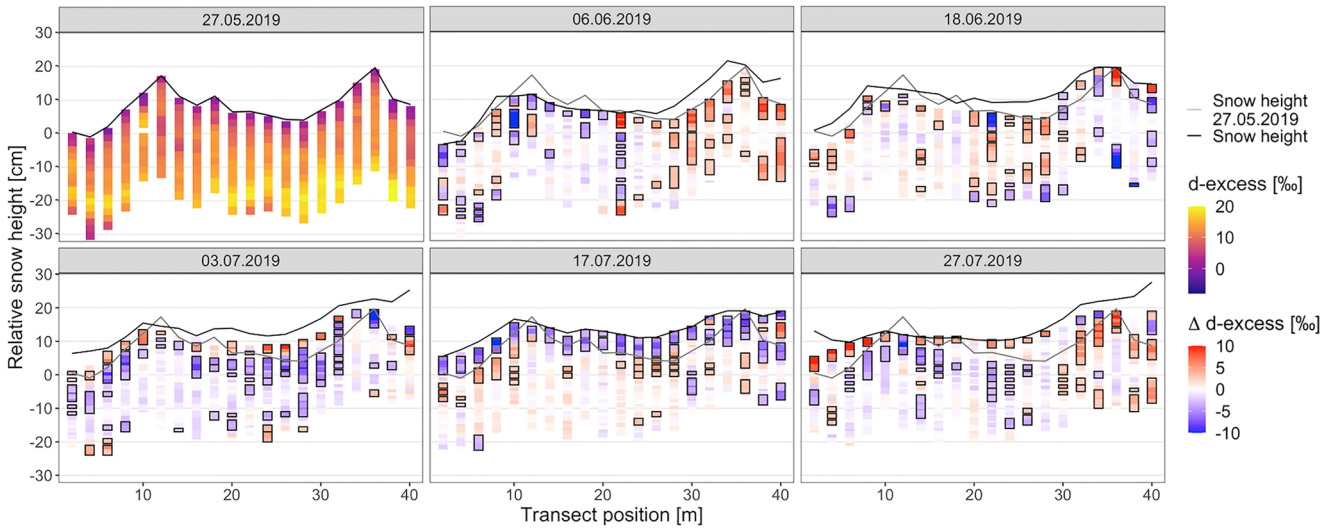

Figure 8. d-excess data for the first sampling on 27 May and differences in d-excess (Δ d-excess) from one sampling to the next for all other sampling dates. Only depths are considered which had snow during both sampling events, hence, there is no difference for areas where new snow was deposited or snow was eroded during a 2-week period. Black squares indicate significant changes. The black line indicates the relative snow height for each individual sampling day and the gray line is the snow height of the first sampling day, 27 May 2019. Contrary to Figure 7, we show the difference, the Δ values, for all snow samples that were present on consecutive sampling days.

apply the same method to estimate a threshold for local significance as for $\delta^{18}O$ and consider significant changes larger than ±2 SD (i.e., 2.5‰). For the samplings on 6 June, 18 June, and 27 July, the difference in d-excess, Δ d-excess, between two sampling events for all overlapping positions on both respective days shows no clear trend throughout the entire snow column although some changes are significant (Figure 8). The period between 18 June and 17 July 2019, however, shows a spatially homogeneous behavior with essentially opposite changes in the d-excess parameter with positive changes in the near-surface snow between 18 June and 3 July, followed by negative Δ d-excess values toward 17 July.

4. Discussion

We present a new approach to study the buildup of the isotopic signal in the snow column and its post-depositional modifications at and beneath the surface, combining elevation models from SfM photogrammetry and a transect of snow profiles sampled throughout a 2-months field season.

4.1. Evolution of the Snow Surface

Our new DEM data confirms the results found in a similar transect in the previous year (Zuhr et al., 2021), showing that the snow deposition is irregular in space, ranging from a net negative change (erosion) up to an increase of 14 cm (Figure 3) throughout the season. Similar to 2018, the snow surface became generally flatter during the season in 2019, as troughs were filled up and peaks eroded, resulting in a negative correlation ($r = -0.53$, $p < 0.05$) between the initial snow height and the amount of accumulated snow. This supports that the observed pattern was not a specific feature of the season in 2018 but is a systematic behavior for this area in northeast Greenland, similar to findings from other locations with comparable accumulation characteristics in central Greenland (Albert & Hawley, 2002; Kuhns et al., 1997).

4.2. Two-Dimensional View of $\delta^{18}O$ in the Snow

Our two-dimensional profiles (40 m wide and 30 cm deep) of the isotopic variations (Figure 5) provide the first visualization of the $\delta^{18}O$ signal and stratigraphic noise in snow from the GrIS, similar to the findings from snow trenches in Antarctica (Münch et al., 2016, 2017). We find a pattern of top-down enriched-depleted-enriched isotopic composition, presumably indicative for seasonal layering in addition to horizontal isotopic variability which is caused by local stratigraphic noise. While our profiles are too short to quantify the stratigraphic noise,

a very rough estimation of the SNR variance ratio $\left(\mathrm{SNR} = \left(\sigma_v^2 - \sigma_h^2\right)/\sigma_h^2\right)$, comparing the horizontal $\left(\sigma_h^2\right)$ and vertical $\left(\sigma_v^2\right)$ variance (Münch et al., 2016), results in a SNR of 1.8. This is consistent with the typical SNR values documented for Greenlandic sites that range from 1 to 3 (Fisher et al., 1985) and considerably higher than the SNR of 0.6 found in the trench studies in Antarctica from an area with approximately half of the annual accumulation than our study site (Münch et al., 2016, 2017). The lower stratigraphic noise (thus higher SNR) at our site compared to Antarctica is expected as it is mainly determined by the ratio of the annual layer thickness (about twice as high at this study site) relative to the thickness of snow surface undulations (similar at both sites) (Fisher et al., 1985). As a first approximation, this means that fewer profiles have to be averaged in Greenland to yield the same information density compared to typical ice core sites in Antarctica.

However, the two-dimensional δ^{18}O profiles also demonstrate that single vertical profiles, such as firn cores, can miss individual seasons, as observed in this study by a missing winter layer at transect position 32 m as well as reported from single ion records (Gfeller et al., 2014). On the contrary, seasons can be strongly overrepresented in other close-by profiles, for example, in the profile at 36 m (Figure 5).

4.3. The Snow d-excess Signal and Its Influencing Parameters

Conventionally, the d-excess parameter is interpreted as a moisture source region proxy (Landais et al., 2021). However, post-depositional processes, such as the latent heat flux, wind pumping, or metamorphism, are reported to lead to isotopic exchange between the atmosphere, surface snow, and interstitial air within the snow column (e.g., Casado et al., 2021; Ebner et al., 2017; Sokratov & Golubev, 2009; Steen-Larsen et al., 2014; Town et al., 2008). These processes are determined by prevailing environmental conditions at the study site and are most visible in the d-excess parameter due to their non-equilibrium nature.

We focus here on the presented case study of observed spatially homogenous trends in the 2 weeks before and after the sampling on 3 July 2019. They were fundamentally different during these two 2-week periods, as reflected in the contrasting Δ d-excess signals in the snow. Environmental conditions during our observation period were analyzed and described in Harris Stuart et al. (2021), Wahl et al. (2021), and Wahl et al. (2022). The latent heat flux is largest during the period from 18 June to 17 July with a 2-week cumulative flux of ~2,400 W m^{-2} representing peak summer sublimation values (Wahl et al., 2021) (Table S1 in Supporting Information S1). However, the period between 18 June and 3 July was additionally characterized by several snowfall and -drift events (Figure 2) and a mean snow height increase of 3.3 cm (Table S1 in Supporting Information S1). During the following 2 weeks until 17 July, low to moderate wind speeds prevailed and only small changes in snow depth were observed (Figure 8, Table S1 in Supporting Information S1). For the period between 3 and 17 July, Harris Stuart et al. (2021) analyzed a different isotope data set from the same study site and found a decrease in d-excess without changes in δ^{18}O, similar to our observations (Figure S2 in Supporting Information S1). They also report two SSA decrease events during this period potentially related to post-depositional processes, such as vapor-snow exchange.

4.4. Buildup of the Snowpack Isotopic Signal

The isotopic signature in snow and firn profiles has previously been interpreted to reflect the temporal development of the isotopic signature of snowfall. However, the signal at a specific depth is influenced by the interplay between spatially variable processes, such as snow accumulation, redistribution (e.g., Ekaykin et al., 2004; Picard et al., 2019) as well as post-depositional modifications at the surface (e.g., Hughes et al., 2021; Steen-Larsen et al., 2014; Wahl et al., 2022) and within the upper snowpack (e.g., Casado et al., 2021; Johnsen, 1977). To shed light on these processes at and beneath the surface, we make use of the two-dimensional isotopic data set and investigate the signal deposition and its subsequent development through time.

The first order pattern, which is visible when averaging across all δ^{18}O profiles to minimize the stratigraphic noise (Figure 4), is in agreement with the traditional perception of a downward movement ("advection") of the depleted winter layer throughout the season as more isotopically enriched summer snow is deposited at the top. Taking into account the respective snow height of each of the spatially distributed profiles (Figure 5) confirms, that the downward advection of the winter layer is caused by the snow accumulation as the isotope profiles, accounting for the elevation changes, remains largely constant through time below the layer affected by accumulation and erosion.

To test for systematic changes in the isotopic composition of the snow column through time, for example, by forced ventilation (Ebner et al., 2017; Town et al., 2008), we analyzed the temporal δ^{18}O anomalies in the

two-dimensional snow transect (Figure 7). This comparison is limited by the magnitude of expected variations caused by the spatial change of the sampling locations between consecutive samplings. We were, thus, only able to separate temporal changes larger than 2.9‰ from this spatial sampling effect. Given this limitation, our study did not indicate significant alterations below 10 cm depth throughout the 2-months period. However, we found few changes closer to the surface that might be related to isotopic diffusion.

During the summer season, the changes at the surface were characterized by a spatially unequal deposition of warmer, isotopically enriched snow (Figure 6). To see which signal we would expect in the simplest case without post-depositional processes or snowdrift, we constructed a model in which we piled up layers according to the topographical changes with a signal representing the respective daily air temperature. The visual comparison to the observed isotope signature in the surface snow shows that, while the general characteristics of higher $\delta^{18}O$ values corresponding to higher temperatures are captured (described in chapter 3.4), there are also some differences. A thin layer of isotopically depleted snow between 30 and 40 m along the transect was deposited between the first and second sampling and persisted throughout the summer season (Figure 6a). This layer is also represented in the simulation by cold temperatures (Figure 6b). In contrast, the alternating sequence of high and low isotopic values between 0 and 6 m is not shown in the simulation.

This mismatch can have several reasons. One reason could be the quality and temporal gaps in the DEMs as for some days the low visual contrast of the flat surface did not allow a faithful reconstruction of the snow height. However, the largest gap between consecutive DEMs is 3 days. Moreover, Zuhr et al. (2021) investigated in detail the uncertainties of the photogrammetry method and concluded that the observed magnitude of snow height changes is larger than the uncertainty of 1.3 cm. For future studies, improvements in the DEM recovery rate, for example, by using infrared filters (Bühler et al., 2017), or the use of other DEM generating methods, such as laser scanners (Picard et al., 2019), could reduce these uncertainties. Zuhr et al. (2021) also showed a significant negative correlation between the mean daily wind speed and the mean daily snow height change and with the temporal snow height evolution in this study, it seems to be a persistent behavior of the summer snow surface at EastGRIP. This patchy deposition of drifting snow at the surface can substantially contribute to accumulation at one site and might lead to the deposition of snow at another site containing an environmental fingerprint from another location (Ekaykin et al., 2002; Picard et al., 2019). Summer wind conditions exceeding typical thresholds for snowdrift (e.g., 6 m s^{-1} for daily averaged wind speed, Figure 2a) favor substantial snowdrift that affects surface structures (Zuhr et al., 2021) as well as the development of the isotopic layering.

Besides these rather mechanical contributions, additional modifications of the snow's isotopic signature due to post-depositional processes, such as vapor-snow exchange, at the very surface are found to imprint a climate signal into the surface layer during precipitation-free periods in the summer (Casado et al., 2021; Hughes et al., 2021; Wahl et al., 2021, 2022). Sublimation experiments from the same study site report that the isotopic composition within the top few centimeters is affected by the atmospheric diurnal temperature cycle (Hughes et al., 2021) with considerable contribution of isotopic fractionation during sublimation to the observed day-to-day variability (Wahl et al., 2022). Moreover, Harris Stuart et al. (2021) documented significant changes in the d-excess signal of the surface snow following precipitation events, effectively masking the initial precipitation isotopic composition. Following these studies, the presented analysis of d-excess values compared to prevailing environmental conditions suggests that the observed changes in the 2-week period after 3 July 2019 (Figure 8) is a local signal, likely caused by a sublimation-induced decrease in d-excess as shown in numerous laboratory and observational studies (e.g., Casado et al., 2021; Hughes et al., 2021; Madsen et al., 2019; Sokratov & Golubev, 2009). While near-surface $\delta^{18}O$ stays almost constant between 3 and 17 July, the mean d-excess decreases up to 5‰ (Figure S2 in Supporting Information S1) suggesting that local post-depositional processes considerably contribute to the imprint of climatic conditions. Thus, the observed d-excess signature is a result of the entire snowpack buildup, that is, of the processes occurring between precipitation events; however, unambiguous and universal conclusions are difficult due to spatial heterogeneity throughout the season and complex contribution of different post-depositional and depositional processes between the sampling events.

Repeating the study, ideally with a more frequent sampling interval than applied here to also cover snowfall- and erosion-free periods, would allow for a better detection of post-depositional changes at and near the surface. The noise from the spatial shift of sampling locations should be reduced to allow testing for reliable analyses of post-depositional alterations. This could be achieved with optimized sampling schemes that enable shorter distances between successive sampling positions. In addition, combining our study approach with sampling and

measurements of the isotopic composition of snowfall and drifted snow would allow us to perform more detailed simulations and to compare the skill of simulations to our measurements including or excluding processes, such as sublimation. The question of the driving processes that ultimately determine the isotopic signal remains, therefore, open but points to a combination of the precipitated isotope signal altered by post-depositional processes, such as vapor-snow exchange. Snowpack models, which consider exchanges with the vapor (Wahl et al., 2022) and physical modifications of the snow surface (Libois et al., 2014), could be used to estimate expected changes helping to develop new study designs.

5. Conclusion

We investigated the temporal evolution of the snow surface in northeast Greenland based on snow height information and two-dimensional snow isotope transects. We identified uneven snow deposition as the main driver for buildup and preservation of stratigraphic noise, confirming the conceptual model by Fisher et al. (1985). In addition, the isotopic data revealed that the climatic signal is mainly introduced at the surface by either snowfall or depositional and post-depositional modifications of the surface and sub-surface layers, such as snowdrift and vapor-snow exchange. Changes in $\delta^{18}O$ below ~10 cm were not significant and, therefore, cannot confirm wind pumping or other processes altering the properties of buried snow, while confirming similar studies in Antarctic snow (Münch et al., 2016). Significant changes in d-excess were observed throughout the snowpack but were most prominent and heterogenous in the surface layer. These observations clearly show local processes influencing the d-excess signal and masking the source region information. However, the spatial variability limited the ability to detect significant changes smaller than 2.9‰ for $\delta^{18}O$ and 2.5‰ for d-excess with the current setup during a 2-months summer period.

We have shown that this study design, which combines snow height information with isotope records, allows quantification of the buildup of the snow column. In a next step, extending the gained knowledge through refined simulations of the expected isotopic composition of the snow column, could allow an evaluation of the presented snowpack buildup. Ideally, these simulations should also include post-depositional changes, such as sublimation and redistribution, as we find evidence that the vapor-snow exchange processes alter the isotopic composition, especially the d-excess signal at the surface.

Further optimizations of the study design with, for example, a higher temporal resolution to capture periods without snowfall or improved devices to reduce the spatial shift between consecutive sampling positions, should improve the investigation of the post-depositional changes. Additionally, improvements in the measurement of the isotopic composition in snowfall (Kopec et al., 2019; Stenni et al., 2016) and a method to differentiate between snowdrift and fresh snow are needed to refine our understanding and simulations of the signal formation. Repeating this or improved study designs in regions with different environmental conditions, such as the low accumulation regions on the East Antarctic Plateau or other areas in Greenland with higher accumulation rates, should enhance our overall understanding of the climatic signal contained in stable water isotopes in polar firn and ice cores.

Data Availability Statement

The DEM generation was carried out using the software Agisoft Metashape (version 1.8.3, retrieved from https://www.agisoft.com/downloads/installer/, last accessed: 19 May 2022). All snow height information and isotope data are accessible in the PANGAEA data repository. The digital elevation models are available as Zuhr et al. (2023a) and the detailed analyzed snow height information as Zuhr et al. (2023b). The isotope data are available as Zuhr et al. (2022). Additionally used data of environmental conditions are used from Steen-Larsen and Wahl (2020, 2021). All numerical analyses were carried out by using the software R: a language and environment for statistical computing.

Acknowledgments
This is a contribution to the SPACE ERC project. This work has received funding from the European Research Council (ERC) under the European Union's Horizon 2020 research and innovation program Starting Grant SPACE (Grant 716092) and Starting Grant SNOWISO (Grant 759526). EastGRIP is directed and organized by the Centre for Ice and Climate at the Niels Bohr Institute, University of Copenhagen. It is supported by funding agencies and institutions in Denmark (A. P. Møller Foundation, University of Copenhagen), USA (US National Science Foundation, Office of Polar Programs), Germany (Alfred Wegener Institute, Helmholtz Centre for Polar and Marine Research), Japan (National Institute of Polar Research and Arctic Challenge for Sustainability), Norway (University of Bergen and Trond Mohn Foundation), Switzerland (Swiss National Science Foundation), France (French Polar Institute Paul-Emile Victor, Institute for Geosciences and Environmental research), Canada (University of Manitoba), and China (Chinese Academy of Sciences and Beijing Normal University). The authors further thank Thomas Münch for helpful discussions during the planning of the study and providing the Greenland map, the AWI workshop for the construction of the photogrammetry equipment and everyone that supported this study during the field campaign and the generation of the DEMs. The authors further thank Mikaela Weiner for supporting the measurements in the Stable Isotope Facility at the Alfred Wegener Institute as well as the editor and the two reviewer for supporting and improving this article. Open Access funding enabled and organized by Projekt DEAL.

References

Albert, M. R., & Hawley, R. L. (2002). Seasonal changes in snow surface roughness characteristics at Summit, Greenland: Implications for snow and firn ventilation. *Annals of Glaciology*, *35*, 510–514. https://doi.org/10.3189/172756402781816591

Barnes, P. R. F., Wolff, E. W., & Mulvaney, R. (2006). A 44 kyr paleoroughness record of the Antarctic surface. *Journal of Geophysical Research*, *111*(D3), D03102. https://doi.org/10.1029/2005JD006349

Brook, E. J., & Buizert, C. (2018). Antarctic and global climate history viewed from ice cores. *Nature*, *558*(7709), 200–208. https://doi.org/10.1038/s41586-018-0172-5

Bühler, Y., Adams, M. S., Stoffel, A., & Boesch, R. (2017). Photogrammetric reconstruction of homogenous snow surfaces in alpine terrain applying near-infrared UAS imagery. *International Journal of Remote Sensing*, *38*(8–10), 3135–3158. https://doi.org/10.1080/01431161.2016.1275060

Casado, M., Landais, A., Picard, G., Arnaud, L., Dreossi, G., Stenni, B., & Prié, F. (2021). Water isotopic signature of surface snow metamorphism in Antarctica. *Geophysical Research Letters*, *48*(17), e2021GL093382. https://doi.org/10.1029/2021GL093382

Craig, H. (1961). Standard for reporting concentrations of deuterium and oxygen-18 in natural waters. *Science*, *133*(3467), 1833–1834. https://doi.org/10.1126/science.133.3467.1833

Dansgaard, W. (1964). Stable isotopes in precipitation. *Tellus*, *16*(4), 436–468. https://doi.org/10.3402/tellusa.v16i4.8993

Ebner, P. P., Steen-Larsen, H. C., Stenni, B., Schneebeli, M., & Steinfeld, A. (2017). Experimental observation of transient $\delta^{18}O$ interaction between snow and advective airflow under various temperature gradient conditions. *The Cryosphere*, *11*(4), 1733–1743. https://doi.org/10.5194/tc-11-1733-2017

Ekaykin, A. A., Lipenkov, V. Y., Barkov, N. I., Petit, J. R., & Masson-Delmotte, V. (2002). Spatial and temporal variability in isotope composition of recent snow in the vicinity of Vostok station, Antarctica: Implications for ice-core record interpretation. *Annals of Glaciology*, *35*, 181–186. https://doi.org/10.3189/172756402781816726

Ekaykin, A. A., Lipenkov, V. Y., Kuzmina, I. N., Petit, J. R., Masson-Delmotte, V., & Johnsen, S. J. (2004). The changes in isotope composition and accumulation of snow at Vostok station, East Antarctica, over the past 200 years. *Annals of Glaciology*, *39*, 569–575. https://doi.org/10.3189/172756404781814348

EPICA Community Members. (2004). Eight glacial cycles from an Antarctic ice core. *Nature*, *429*(6992), 623–628. https://doi.org/10.1038/nature02599

Fausto, R. S., van As, D., Mankoff, K. D., Vandecrux, B., Citterio, M., Ahlstrøm, A. P., et al. (2021). Programme for Monitoring of the Greenland Ice Sheet (PROMICE) automatic weather station data. *Earth System Science Data*, *13*(8), 3819–3845. https://doi.org/10.5194/essd-13-3819-2021

Fisher, D. A., Reeh, N., & Clausen, H. B. (1985). Stratigraphic noise in time series derived from ice cores. *Annals of Glaciology*, *7*(1), 76–83. https://doi.org/10.1017/S0260305500005942

Gfeller, G., Fischer, H., Bigler, M., Schüpbach, S., Leuenberger, D., & Mini, O. (2014). Representativeness and seasonality of major ion records derived from NEEM firn cores. *The Cryosphere*, *8*(5), 1855–1870. https://doi.org/10.5194/tc-8-1855-2014

Gonfiantini, R. (1978). Standards for stable isotope measurements in natural compounds. *Nature*, *271*(5645), 534–536. https://doi.org/10.1038/271534a0

Graf, W., Oerter, H., Reinwarth, O., Stichler, W., Wilhelms, F., Miller, H., & Mulvaney, R. (2002). Stable-isotope records from Dronning Maud Land, Antarctica. *Annals of Glaciology*, *35*(1), 195–201. https://doi.org/10.3189/172756402781816492

Harris Stuart, R., Faber, A.-K., Wahl, S., Hörhold, M., Kipfstuhl, S., Vasskog, K., et al. (2021). Exploring the role of snow metamorphism on the isotopic composition of the surface snow at EastGRIP. *The Cryosphere Discuss*. [preprint]. https://doi.org/10.5194/tc-2021-344

Hughes, A. G., Wahl, S., Jones, T. R., Zuhr, A., Hörhold, M., White, J. W. C., & Steen-Larsen, H. C. (2021). The role of sublimation as a driver of climate signals in the water isotope content of surface snow: Laboratory and field experimental results. *The Cryosphere*, *15*(10), 4949–4974. https://doi.org/10.5194/tc-15-4949-2021

James, M. R., & Robson, S. (2012). Straightforward reconstruction of 3D surfaces and topography with a camera: Accuracy and geoscience application. *Journal of Geophysical Research*, *117*(F3),F03017. https://doi.org/10.1029/2011JF002289

Johnsen, S. J. (1977). Stable isotope homogenization of polar firn and ice. In *Isotopes and impurities in snow and ice, no. 118* (pp. 210–219).

Johnsen, S. J., Clausen, H. B., Cuffey, K. M., Hoffmann, G., Schwander, J., & Creyts, T. (2000). Diffusion of stable isotopes in polar firn and ice: The isotope effect in firn diffusion. In T. Hondoh (Ed.), *Physics of ice core records* (Vol. 159, pp. 121–140). Sapporo.

Jouzel, J., Vimeux, F., Caillon, N., Delaygue, G., Hoffmann, G., Masson-Delmotte, V., & Parrenin, F. (2003). Magnitude of isotope/temperature scaling for interpretation of central Antarctic ice cores. *Journal of Geophysical Research*, *108*(D12), 4361. https://doi.org/10.1029/2002JD002677

Karlöf, L., Winebrenner, D. P., & Percival, D. B. (2006). How representative is a time series derived from a firn core? A study at a low-accumulation site on the Antarctic plateau. *Journal of Geophysical Research*, *111*(F4), F04001. https://doi.org/10.1029/2006JF000552

Karlsson, N. B., Razik, S., Hörhold, M., Winter, A., Steinhage, D., Binder, T., & Eisen, O. (2020). Surface accumulation in Northern Central Greenland during the last 300 years. *Annals of Glaciology*, *61*(81), 214–224. https://doi.org/10.1017/aog.2020.30

Kopec, B. G., Feng, X., Posmentier, E. S., & Sonder, L. J. (2019). Seasonal deuterium excess variations of precipitation at Summit, Greenland, and their climatological significance. *Journal of Geophysical Research: Atmospheres*, *124*(1), 72–91. https://doi.org/10.1029/2018JD028750

Kuhns, H., Davidson, C., Dibb, J., Stearns, C., Bergin, M., & Jaffrezo, J.-L. (1997). Temporal and spatial variability of snow accumulation in central Greenland. *Journal of Geophysical Research*, *102*(D25), 30059–30068. https://doi.org/10.1029/97JD02760

Laepple, T., Hörhold, M., Münch, T., Freitag, J., Wegner, A., & Kipfstuhl, S. (2016). Layering of surface snow and firn at Kohnen Station, Antarctica: Noise or seasonal signal? *Journal of Geophysical Research: Earth Surface*, *121*(10), 1849–1860. https://doi.org/10.1002/2016JF003919

Landais, A., Stenni, B., Masson-Delmotte, V., Jouzel, J., Cauquoin, A., Fourré, E., et al. (2021). Interglacial Antarctic–Southern Ocean climate decoupling due to moisture source area shifts. *Nature Geoscience*, *14*(12), 918–923. https://doi.org/10.1038/s41561-021-00856-4

Libois, Q., Picard, G., Arnaud, L., Morin, S., & Brun, E. (2014). Modeling the impact of snow drift on the decameter-scale variability of snow properties on the Antarctic plateau. *Journal of Geophysical Research: Atmospheres*, *119*(20), 11662–11681. https://doi.org/10.1002/2014JD022361

Lorius, C., Merlivat, L., & Hagemann, R. (1969). Variation in the mean deuterium content of precipitations in Antarctica. *Journal of Geophysical Research*, *74*(28), 7027–7031. https://doi.org/10.1029/JC074i028p07027

Madsen, M. V., Steen-Larsen, H. C., Hörhold, M., Box, J., Berben, S. M. P., Capron, E., et al. (2019). Evidence of isotopic fractionation during vapor exchange between the atmosphere and the snow surface in Greenland. *Journal of Geophysical Research: Atmospheres*, *124*(6), 2932–2945. https://doi.org/10.1029/2018JD029619

Merlivat, L., & Jouzel, J. (1979). Global climatic interpretation of the deuterium-oxygen 18 relationship for precipitation. *Journal of Geophysical Research*, *84*(C8), 5029. https://doi.org/10.1029/JC084iC08p05029

Münch, T., Kipfstuhl, S., Freitag, J., Meyer, H., & Laepple, T. (2016). Regional climate signal vs. local noise: A two-dimensional view of water isotopes in Antarctic firn at Kohnen Station, Dronning Maud Land. *Climate of the Past*, *12*(7), 1565–1581. https://doi.org/10.5194/cp-12-1565-2016

Münch, T., Kipfstuhl, S., Freitag, J., Meyer, H., & Laepple, T. (2017). Constraints on post-depositional isotope modifications in East Antarctic firn from analysing temporal changes of isotope profiles. *The Cryosphere*, *11*(5), 2175–2188. https://doi.org/10.5194/tc-11-2175-2017

Münch, T., & Laepple, T. (2018). What climate signal is contained in decadal-to centennial-scale isotope variations from Antarctic ice cores? *Climate of the Past*, *14*(12), 2053–2070. https://doi.org/10.5194/cp-14-2053-2018

Pfahl, S., & Sodemann, H. (2014). What controls deuterium excess in global precipitation? *Climate of the Past*, *10*(2), 771–781. https://doi.org/10.5194/cp-10-771-2014

Picard, G., Arnaud, L., Caneill, R., Lefebvre, E., & Lamare, M. (2019). Observation of the process of snow accumulation on the Antarctic Plateau by time lapse laser scanning. *The Cryosphere*, *13*(7), 1983–1999. https://doi.org/10.5194/tc-13-1983-2019

Ritter, F., Steen-Larsen, H. C., Werner, M., Masson-Delmotte, V., Orsi, A., Behrens, M., et al. (2016). Isotopic exchange on the diurnal scale between near-surface snow and lower atmospheric water vapor at Kohnen station, East Antarctica. *The Cryosphere*, *10*(4), 1647–1663. https://doi.org/10.5194/tc-10-1647-2016

Schaller, C. F., Freitag, J., Kipfstuhl, S., Laepple, T., Steen-Larsen, H. C., & Eisen, O. (2016). A representative density profile of the North Greenland snowpack. *The Cryosphere*, *10*(5), 1991–2002. https://doi.org/10.5194/tc-10-1991-2016

Sokratov, S. A., & Golubev, V. N. (2009). Snow isotopic content change by sublimation. *Journal of Glaciology*, *55*(193), 823–828. https://doi.org/10.3189/002214309790152456

Steen-Larsen, H. C., Masson-Delmotte, V., Hirabayashi, M., Winkler, R., Satow, K., Prié, F., et al. (2014). What controls the isotopic composition of Greenland surface snow? *Climate of the Past*, *10*(1), 377–392. https://doi.org/10.5194/cp-10-377-2014

Steen-Larsen, H. C., & Wahl, S. (2020). 2 m wind speed, wind direction and air temperature at EastGRIP site on Greenland Ice Sheet, summer 2019 [Dataset]. Pangaea. https://doi.org/10.1594/PANGAEA.925618

Steen-Larsen, H. C., & Wahl, S. (2021). 2 m processed sensible and latent heat flux, friction velocity and stability at EastGRIP site on Greenland Ice Sheet, summer 2019 [Dataset]. Pangaea. https://doi.org/10.1594/PANGAEA.928827

Stenni, B., Scarchilli, C., Masson-Delmotte, V., Schlosser, E., Ciardini, V., Dreossi, G., et al. (2016). Three-year monitoring of stable isotopes of precipitation at Concordia Station, East Antarctica. *The Cryosphere*, *10*(5), 2415–2428. https://doi.org/10.5194/tc-10-2415-2016

Town, M. S., Warren, S. G., Walden, V. P., & Waddington, E. D. (2008). Effect of atmospheric water vapor on modification of stable isotopes in near-surface snow on ice sheets. *Journal of Geophysical Research*, *113*, D24303. https://doi.org/10.1029/2008JD009852

Vallelonga, P., Christianson, K., Alley, R. B., Anandakrishnan, S., Christian, J. E. M., Dahl-Jensen, D., et al. (2014). Initial results from geophysical surveys and shallow coring of the Northeast Greenland Ice Stream (NEGIS). *The Cryosphere*, *8*(4), 1275–1287. https://doi.org/10.5194/tc-8-1275-2014

van Geldern, R., & Barth, J. A. (2012). Optimization of instrument setup and post-run corrections for oxygen and hydrogen stable isotope measurements of water by isotope ratio infrared spectroscopy (IRIS). *Limnology and Oceanography: Methods*, *10*(12), 1024–1036. https://doi.org/10.4319/lom.2012.10.1024

Wahl, S., Steen-Larsen, H. C., Hughes, A. G., Dietrich, L. J., Zuhr, A., Behrens, M., et al. (2022). Atmosphere-snow exchange explains surface snow isotope variability. *Geophysical Research Letters*, *49*(20), e2022GL099529. https://doi.org/10.1029/2022GL099529

Wahl, S., Steen-Larsen, H. C., Reuder, J., & Hörhold, M. (2021). Quantifying the stable water isotopologue exchange between the snow surface and lower atmosphere by direct flux measurements. *Journal of Geophysical Research: Atmospheres*, *126*(13), e2020JD034400. https://doi.org/10.1029/2020JD034400

Weinhart, A. H., Freitag, J., Hörhold, M., Kipfstuhl, S., & Eisen, O. (2020). Representative surface snow density on the East Antarctic Plateau. *The Cryosphere*, *14*(11), 3663–3685. https://doi.org/10.5194/tc-14-3663-2020

Wolff, E. W., Cook, E., Barnes, P. R. F., & Mulvaney, R. (2005). Signal variability in replicate ice cores. *Journal of Glaciology*, *51*(174), 462–468. https://doi.org/10.3189/172756505781829197

Zuhr, A. M., Münch, T., Steen-Larsen, H. C., Hörhold, M., & Laepple, T. (2021). Local-scale deposition of surface snow on the Greenland Ice Sheet. *The Cryosphere*, *15*(10), 4873–4900. https://doi.org/10.5194/tc-15-4873-2021

Zuhr, A. M., Wahl, S., Steen-Larsen, H. C., Meyer, H., Faber, A.-K., & Laepple, T. (2023a). Digital Elevation Models from the summer season 2019 at the EastGRIP deep drilling site [Dataset]. Pangaea. https://doi.org/10.1594/PANGAEA.954944

Zuhr, A. M., Wahl, S., Steen-Larsen, H. C., Meyer, H., Faber, A.-K., & Laepple, T. (2023b). Snow height information derived from Digital Elevation Models from the summer season 2019 at the EastGRIP deep drilling site [Dataset]. Pangaea. https://doi.org/10.1594/PANGAEA.954945

Zuhr, A. M., Wahl, S., Steen-Larsen, H. C., Meyer, H., Weiner, M., & Laepple, T. (2022). Stable water isotopes from repeated snow profile sampling during the summer season 2019 at the EastGRIP deep drilling site [Dataset]. Pangaea. https://doi.org/10.1594/PANGAEA.951583